



## Unveiling and Driving Hidden Resonances with High-Fluence, High-Intensity X-Ray Pulses

E. P. Kanter,<sup>1,\*</sup> B. Krässig,<sup>1</sup> Y. Li,<sup>1</sup> A. M. March,<sup>1</sup> P. Ho,<sup>1</sup> N. Rohringer,<sup>2,3,4,5,†</sup> R. Santra,<sup>1,6,7,5,‡</sup> S. H. Southworth,<sup>1</sup> L. F. DiMauro,<sup>8</sup> G. Doumy,<sup>8,§</sup> C. A. Roedig,<sup>8</sup> N. Berrah,<sup>9</sup> L. Fang,<sup>9</sup> M. Hoener,<sup>9</sup> P. H. Bucksbaum,<sup>10</sup> S. Ghimire,<sup>10</sup> D. A. Reis,<sup>10</sup> J. D. Bozek,<sup>11</sup> C. Bostedt,<sup>11</sup> M. Messerschmidt,<sup>11</sup> and L. Young<sup>1,||</sup>

<sup>1</sup>Argonne National Laboratory, Argonne, Illinois 60439, USA

<sup>2</sup>Lawrence Livermore National Laboratory, Livermore, California 94551, USA

<sup>3</sup>Max Planck Institute for the Physics of Complex Systems, 01187 Dresden, Germany

<sup>4</sup>Max Planck Advanced Study Group, Center for Free-Electron Laser Science, DESY, Notkestraße 85, 22607 Hamburg, Germany

<sup>5</sup>Kavli Institute for Theoretical Physics, University of California, Santa Barbara, California 93106, USA

<sup>6</sup>Center for Free-Electron Laser Science, DESY, Notkestraße 85, 22607 Hamburg, Germany

<sup>7</sup>Department of Physics, University of Hamburg, Jungiusstraße 9, 20355 Hamburg, Germany

<sup>8</sup>Ohio State University, Columbus, Ohio 43210, USA

<sup>9</sup>Western Michigan University, Kalamazoo, Michigan 49008, USA

<sup>10</sup>PULSE Center, SLAC, Menlo Park, California 94025, USA

<sup>11</sup>Linac Coherent Light Source, SLAC, Menlo Park, California 94025, USA

(Received 15 June 2011; published 30 November 2011)

We show that high fluence, high-intensity x-ray pulses from the world's first hard x-ray free-electron laser produce nonlinear phenomena that differ dramatically from the linear x-ray–matter interaction processes that are encountered at synchrotron x-ray sources. We use intense x-ray pulses of sub-10-fs duration to first reveal and subsequently drive the  $1s \leftrightarrow 2p$  resonance in singly ionized neon. This photon-driven cycling of an inner-shell electron modifies the Auger decay process, as evidenced by line shape modification. Our work demonstrates the propensity of high-fluence, femtosecond x-ray pulses to alter the target within a single pulse, i.e., to unveil hidden resonances, by cracking open inner shells energetically inaccessible via single-photon absorption, and to consequently trigger damaging electron cascades at unexpectedly low photon energies.

DOI: 10.1103/PhysRevLett.107.233001

PACS numbers: 32.80.Aa, 32.70.Jz, 32.80.Hd, 32.80.Wr

Ultraintense, tunable x-ray pulses recently available from x-ray free-electron lasers (XFELs) [1] increase the intensity and fluence available in a single x-ray pulse up to a billion-fold over that typically available at synchrotron facilities. As a result, XFELs provide a unique opportunity to investigate nonlinear phenomena at short wavelengths. Initial experiments with XFELs demonstrated the most basic nonlinear x-ray process, multiphoton absorption, using photon energies far removed from absorption resonances, first in the extreme ultraviolet [2] and later in the soft x-ray regimes, in atoms [3,4] and molecules [5–7]. The first experiment at the LCLS (Linac Coherent Light Source), the world's first hard x-ray free-electron laser, revealed the ability of a single  $\sim 100$ -fs x-ray pulse, at a fluence of  $\sim 10^{20}$   $\gamma/\text{cm}^2$  to strip a neon atom of all its electrons thereby irrevocably altering the target [3]. Thus, the use of high-fluence, high-intensity x-ray radiation as a controlled probe of atomic, molecular and material properties poses a unique challenge for experimentalists, one where characterization of interaction mechanisms at a fundamental level will play an important role.

These early experiments at LCLS [3–7] all studied photon-matter interactions in a continuum, in principle, far removed from resonances. In this study, we focus on resonant interactions. (Earlier work in the EUV using the FLASH FEL to study laser interactions in rare gases [8,9] at

intensities and fluences up to  $10^{16}$   $\text{W}/\text{cm}^2$  and  $10^{18}$   $\gamma/\text{cm}^2$ , invoked resonances to explain enhanced ion yields, but did not observe multiphoton resonance behavior directly, in contrast to the present study.) Resonances provide interaction strengths that are more than 1000-fold larger than those in the continuum and the ability to selectively address quantum states. Specifically, at extreme intensities approaching  $10^{18}$   $\text{W}/\text{cm}^2$ , Rabi cycling [10,11] can effectively compete with Auger decay [12] and directly modify the branching between decay channels. Here, starting with a neutral neon target, we used ultraintense, high-fluence x-ray pulses from the LCLS to first reveal and subsequently drive the “hidden”  $1s \rightarrow 2p$  resonance in singly ionized neon and thus demonstrate the ability to modify femtosecond Auger decay. Our work illustrates the complexities associated with using ultraintense, high-fluence x-ray pulses as a controlled probe of matter and is a first step toward photonic control of inner-shell electrons.

While considerable effort has been devoted to the control of atomic and molecular processes using ultrafast laser technology to manipulate valence electrons [13–15], active control of inner-shell electron processes is unexplored. There is potential for wide-ranging applications, e.g., inhibition of Auger decay could suppress x-ray radiation damage [16] and modification of inner-shell electronic structure can alter nuclear lifetimes dominated by internal

conversion [17] or electron capture decay [18]. The absence of research is due to the ultrafast nature of inner-shell decay and the lack of a suitably intense radiation source to selectively address inner-shell electron motion on the relevant time scale. With the realization of the LCLS [1] and impending arrival [19–21] of several other x-ray free-electron lasers (XFELs), this longstanding deficiency has been, to some extent, alleviated. However, the properties of present-day XFELs, based on the self amplified spontaneous emission (SASE) mechanism, [22] are not ideal for quantum control experiments. The lack of longitudinal (temporal) coherence prevents the direct observation of Rabi cycling, even in an isolated two-level system. The current situation is not unlike early research with intense optical lasers, where the effects of a strong stochastic field on atomic transitions were considered more than 30 years ago [23,24].

In anticipation of XFELs theoreticians have considered the effects of strong-field excitation of inner-shell resonances [12,25]. The incoherent nature of the SASE excitation pulse of current XFELs causes the mean times between excitation and stimulated emission to fluctuate. Rohringer and Santra (RS) considered the specific question of how such XFEL fields would affect resonant Auger transitions in the x-ray regime [12]. RS showed that although it was impractical to observe the fs-scale Rabi cycling directly, the effect of the excited state population time being shortened by stimulated emission could be observed by the resultant broadening of the Auger emission lines. It is that effect we investigate here.

We chose to study the  $\text{Ne}^+ 1s \rightarrow 2p$  transition, although the quasi-two-level system originally treated [12] was the prominent  $1s \rightarrow 3p$  resonance in Ne. This choice facilitates both theory and experiment because the  $1s - 2p$  resonance is better isolated (more than 70 natural linewidths separated from the next Rydberg excitation,  $1s - 3p$ ), allowing freedom from lineshape distortion [26] and is stronger by  $30\times$  than that Rydberg transition, decreasing the intensity requirements for Rabi cycling. The only experimental drawback is the lack of a  $2p$  hole in the ground state of neon, thus normally “hiding” the resonance. We overcome this by using a single SASE FEL pulse both to prepare the desired state, singly ionized neon containing a  $2p$  hole, and to drive the  $1s \rightarrow 2p$  transition resonantly, as shown in Fig. 1. By using a relatively short FEL pulse we accrue the additional advantage of relatively clean electron spectra in the region of interest. (We previously demonstrated [3] that longer pulses produce photo- and Auger electrons from higher ionization stages significantly complicating the spectra.) Since the energy of the  $1s - 2p$  resonance, 848 eV, lies well below the binding energy of a  $1s$  electron in neutral neon, 870 eV, a single-photon excitation at 848 eV cannot produce a  $1s$  hole without a  $2p$  vacancy and the appearance of Auger electrons is a clear signature of the  $2p$  resonance. A

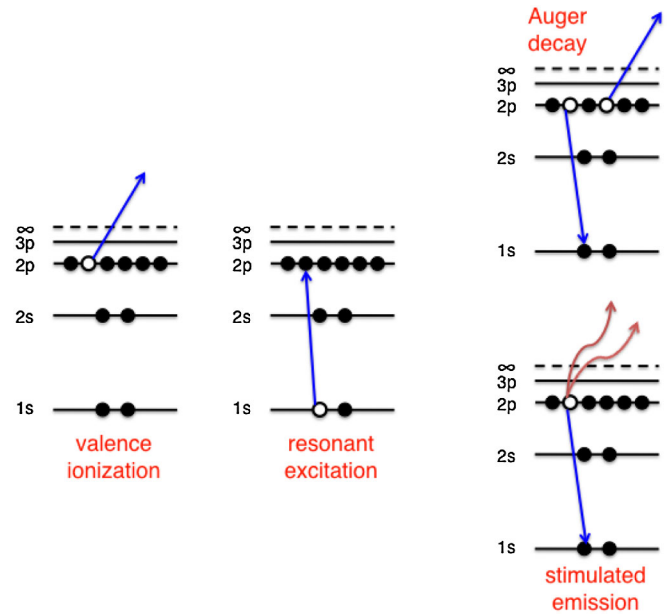


FIG. 1 (color online). Revealing and driving a hidden resonance within a single SASE pulse. An x-ray pulse at 848 eV first strips a  $2p$  electron from Ne to reveal and then excite the  $\text{Ne}^+ 1s \rightarrow 2p$  resonance. Stimulated emission competes with Auger decay to refill the  $1s$  hole. Cycling is terminated by Auger decay which changes the resonance energy.

comparison of the Auger line profiles for resonant (848 eV) and nonresonant (930 eV) excitation with theory then constitutes the evidence for the modification of the Auger decay through Rabi cycling of inner-shell electrons.

We stepped the x-ray energy through the region of interest (840–860 eV), by tuning the electron beam energy of the LCLS, and recorded electron emission spectra at each step. The x-ray pulses (of nominal energy, duration, and focus 0.3 mJ, 8.5 fs, and  $1 \times 2 \mu\text{m}^2$  would yield intensities approaching  $10^{18} \text{ W/cm}^2$ , assuming a beam line transmission of  $\sim 20\%$ ) intersected a Ne gas jet in the High Field Physics chamber. These pulse parameters were confirmed through comparisons of measured charge state distributions with theoretical simulations. [3]

The experimental setup and protocol have been detailed in [3] and references therein. The only significant change was to record the LCLS electron beam energy shot-by-shot in the data stream [1]. This allowed us to characterize the x-ray radiation bandwidth and jitter. Because the x-ray energy,  $E_x$  in eV, is related to the electron energy,  $E_e$  in GeV, by  $E_x = 44.25 E_e^2$ , we could (1) determine the photon energy of individual x-ray pulses to  $\pm 0.1$  eV, and (2) decompose the observed x-ray photon energy spread ( $\sim 0.7\%$ ) into components due to jitter ( $\sim 0.5\%$ ) and intrinsic bandwidth ( $\sim 0.5\%$ )

Electron yields versus incident x-ray energy, corrected on a shot-by-shot basis, are mapped in Fig. 2(a). Only electrons emitted perpendicular to the x-ray polarization

axis are shown, thus suppressing  $2s$  photoelectrons. The  $2p$  photoelectrons disperse linearly with the incident photon energy, forming a prominent diagonal line, whereas the Auger electrons are independent of  $E_x$ , forming vertical lines. Additional higher-lying vertical lines represent Auger decays from higher charge state  $\text{Ne}^{+q}$  ions. Unlabeled diagonal features are photoelectron correlation satellites. The appearance of Auger lines near  $E_x = 848$  eV is a clear signature of the  $1s - 2p$  resonance in  $\text{Ne}^{1+}$  resulting from the valence ionization, resonant excitation sequence shown in Fig. 1.

This resonance is shown in Fig. 2(b), where the  $^1D$  Auger yield is projected onto the x-ray photon energy axis,  $E_x$ . The signature Auger electrons appear only within a few eV of the expected  $1s \rightarrow 2p$  resonance of singly-ionized neon at 848 eV. The small resonance  $\sim 8.5$  eV higher in energy is attributed to the  $1s - 2p$  excitation in doubly-ionized neon ( $2p^{-2} \rightarrow 1s^{-1}2p^{-1}$ ). The data are fit using Voigt profiles with a fixed Lorentzian width of 0.27 eV (corresponding to a lifetime of 2.4 fs) [27,28] and Gaussian FWHM of 5.6 eV. These resonances are not present in the original target and are only revealed as a consequence of sequential valence photoionization at photon energies below the  $1s$ -binding energy of neutral neon, 870 eV. Figure 2(c) shows, for the first three ionization stages the strength and location of hidden absorption resonances that are induced by the high-fluence LCLS pulses. The  $1s \rightarrow 2p$  absorption resonances are enormous ( $10^3$ 's of Mb), roughly 3 orders of magnitude

larger than neutral neon absorption cross sections in this vicinity ( $\sim 10$  kb) arising from valence photoabsorption. (Our simple Hartree-Fock-Slater calculations provide inner-shell transition energies accurate to  $\sim 10$  eV; energetics in extended molecular systems would be more difficult to predict.)

Next, in Fig. 3, we show the Auger line profile off- and on-resonance, as evidence of Rabi cycling. The off-resonant Auger line profile, shown in (a), is used to determine the instrumental function of the electron spectrometer (Gaussian FWHM 0.56 eV). The on-resonance Auger line profile (b), is obtained by projecting electron kinetic energies for incident photon energies within  $\pm 1$  eV of the  $1s - 2p$  resonance energy. The theoretical simulation (an extension of [12] to be published elsewhere) for the resonant Auger line shape, using beam parameters comparable to the experiment, is overlaid. The Auger line profile was averaged over a large ensemble of chaotic x-ray pulses [12] and integrated over the laser spatial profile, (transversely Gaussian with a Rayleigh range of 1.5 mm), and weighted by the spectrometer efficiency and gas density distribution (Gaussian FWHM of 1.6 mm). The agreement is excellent. Panel (c) shows the theoretical simulations for off- and on-resonance excitation prior to convolution with the instrument function, and more clearly demonstrates the effect of the resonant strong-field excitation.

Intensity averaging over the focal volume—a phenomenon common to all single-beam experiments—leads to the

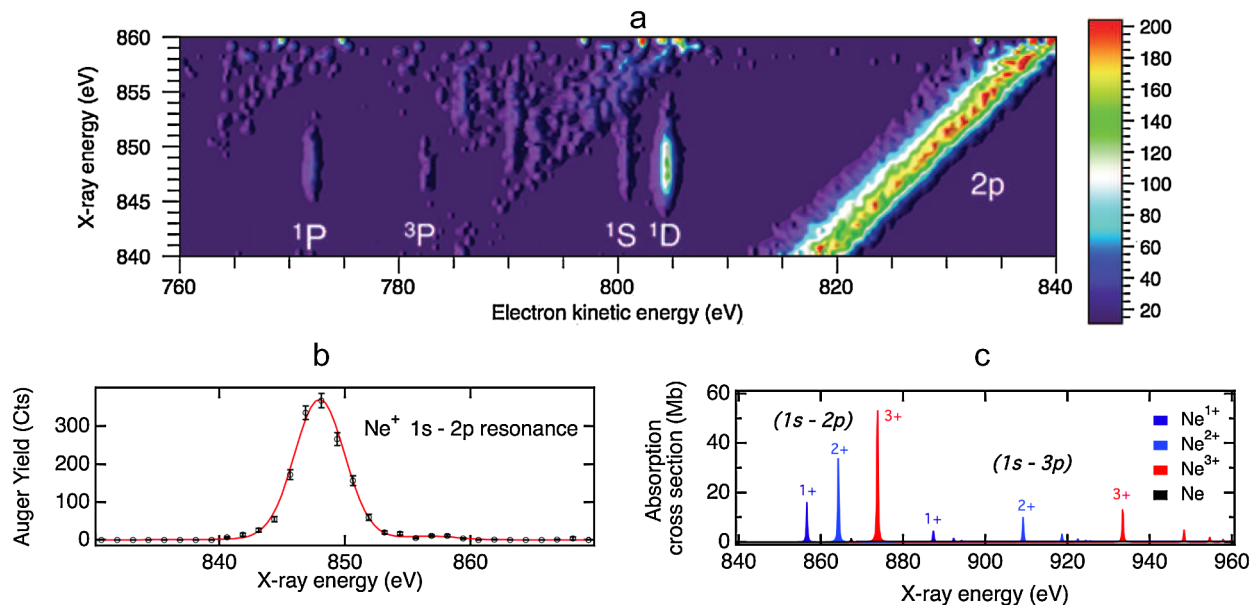


FIG. 2 (color online). (a) Electron emission from Ne vs x-ray energy, observed at  $90^\circ$  to the x-ray polarization axis. Photoelectron lines disperse linearly with photon energy while Auger lines are independent of photon energy [31]. The data are normalized to represent electron yields from x-ray irradiation of 30 Joules/eV. (b)  $^1D$  Auger electron yield as a function of x-ray photon energy. (c) Absorption resonances for higher charge states that can be produced by high-fluence x-ray pulses calculated by the Hartree-Fock-Slater (HFS) method. Neutral Ne resonances, with a maximum cross section of 1.5 Mb, are barely visible, compared to the many ionic resonances.

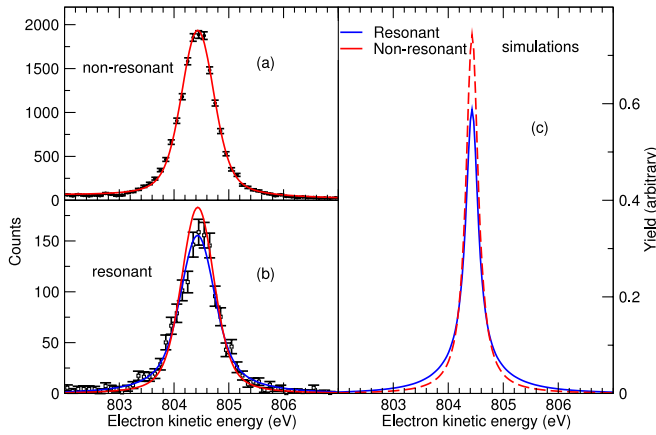


FIG. 3 (color online). Electron kinetic energy spectra of the  $^1D$  Auger line. (a) Nonresonant Auger,  $E_x = 930$  eV. (b) Resonant Auger,  $E_x = 848 \pm 1$  eV. Solid lines are the simulations for the experimental conditions: resonant (blue), nonresonant (red). (c) Simulations of Auger line shape before convolution with the instrumental function. All curves in this figure are normalized to the integrals over the displayed energy region.

rather modest modification of the Auger line profile. The calculated occupation probabilities of the relevant configurations, Fig. 4(a), show that only a small fraction ( $< 2\%$ ) of the sample contributes to the Rabi cycling. Note that as a

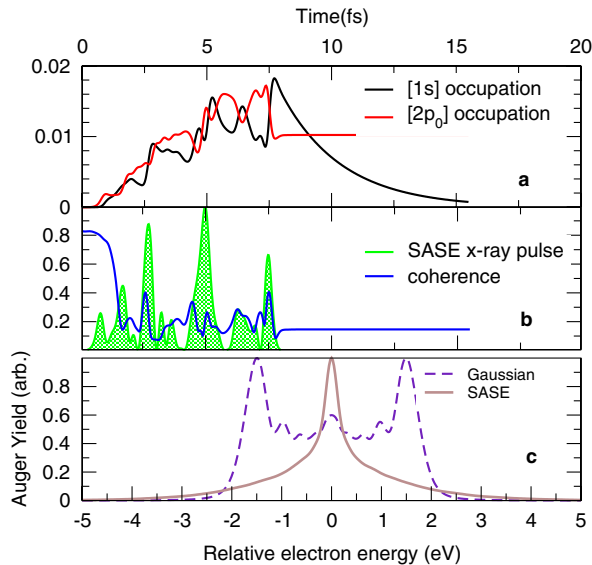


FIG. 4 (color online). Theoretical simulations for resonant  $1s \rightarrow 2p$  excitation of neon with FEL pulses of intensity  $3.5 \times 10^{17}$  W/cm $^2$ . (a) Occupation probabilities for the  $[1s]$  and  $[2p_0]$  vacancy states of the  $\text{Ne}^+$  ion as a function of time for irradiation by the single SASE pulse shown in (b). (b) The degree of coherence between the  $[1s]$  and  $[2p_0]$  vacancy states and SASE pulse profile used in (a) and (b). (c) The resonant Auger line shape generated by an ensemble of SASE pulses (averaged Gaussian temporal profile of 8.5 fs FWHM, 6 eV bandwidth) and a longitudinally coherent Gaussian pulse (8.5 fs FWHM, transform-limited).

consequence of the valence ionization step (Fig. 1), the coherence, defined in this case of a symmetric  $2 \times 2$  density matrix, as the ratio of the magnitude of the off-diagonal matrix element to the square root of the product of the diagonal elements [29], differs from unity even for a single SASE pulse, as shown in Fig. 4(b). With a longitudinally coherent pulse, as should soon be available through self-seeding schemes [30], the situation improves dramatically, as shown in Fig. 4(c), where resonant Auger line profiles are compared for an ensemble of SASE and Gaussian pulses of equal fluence and pulse duration (FWHM). Gaussian pulses drive the resonance more effectively than SASE pulses because the incoherent spikes in the SASE ensemble have a larger effective bandwidth.

While the excitation of the hidden  $1s \rightarrow 2p$  resonance is advantageous here, it is a potential liability for other XFEL experiments. A recent example was the investigation of multiphoton x-ray ionization in which a significant background contribution was attributed to a hidden single-photon resonance in  $\text{Ne}^{7+}$  that allowed sequential valence ionization to compete with direct multiphoton ionization of ground state  $\text{Ne}^{8+}$  to produce  $\text{Ne}^{9+}$  [4].

In summary, this work illustrates the nuances associated with using high-fluence, high-intensity femtosecond x-ray pulses for controlled investigations of material properties. We demonstrate that high-fluence x-ray pulses reveal otherwise hidden resonances through sequential valence ionization. Photoexcitation of these resonances break open inner shells at unexpectedly low photon energies, i.e., below the  $1s$  threshold, and thereby unleash damaging Auger electron cascades. These phenomena must be considered in the design of all future XFEL experiments. We further demonstrate that a strong, incoherent SASE pulse can induce Rabi cycling on a deep inner-shell transition and thus modify Auger decay. Control of inner-shell electron dynamics should be markedly enhanced with soon-to-be-available longitudinally coherent x-ray pulses.

This work was supported by the Chemical Sciences, Geosciences, and Biosciences Division of the Office of Basic Energy Sciences, Office of Science, U.S. Department of Energy (DE-AC02-06CH11357, DE-FG02-04ER15614, DE-FG02-92ER14299). N. R. was supported by the U.S. Department of Energy by Lawrence Livermore National Laboratory (DE-AC52-07NA27344). N. R. and R. S. were supported in part by the National Science Foundation under Grant No. NSF PHY05-51164. M. H. thanks the Alexander von Humboldt Foundation for a Feodor Lynen fellowship. P. H. B., S. G., and D. A. R. were supported through the PULSE Institute, which is jointly funded by the Department of Energy, Basic Energy Sciences, Chemical Sciences, Geosciences and Biosciences Division and Division of Materials Science and Engineering. LCLS is funded by the U.S. Department of Energy's Office of Basic Energy Sciences.

\*kanter@anl.gov

†Present Address: Max Planck Advanced Study Group,  
Center for Free-Electron Laser Science, Hamburg  
22607, Germany.

‡Present Address: Center for Free-Electron Laser Science,  
Hamburg 22607, Germany.

§Present Address: Argonne National Laboratory, Argonne,  
IL 60439, USA.

||young@anl.gov

- [1] P. Emma *et al.*, *Nat. Photon.* **4**, 641 (2010).  
[2] A. A. Sorokin *et al.*, *Phys. Rev. Lett.* **99**, 213002 (2007).  
[3] L. Young *et al.*, *Nature (London)* **466**, 56 (2010).  
[4] G. Doumy *et al.*, *Phys. Rev. Lett.* **106**, 083002 (2011).  
[5] M. Hoener *et al.*, *Phys. Rev. Lett.* **104**, 253002 (2010).  
[6] L. Fang *et al.*, *Phys. Rev. Lett.* **105**, 083005 (2010).  
[7] J. P. Cryan *et al.*, *Phys. Rev. Lett.* **105**, 083004 (2010).  
[8] M. Richter *et al.*, *Phys. Rev. Lett.* **102**, 163002 (2009).  
[9] M. Martins *et al.*, *Phys. Rev. A* **80**, 023411 (2009).  
[10] I. I. Rabi, *Phys. Rev.* **51**, 652 (1937).  
[11] I. I. Rabi *et al.*, *Phys. Rev.* **53**, 318 (1938).  
[12] N. Rohringer and R. Santra, *Phys. Rev. A* **77**, 053404 (2008).  
[13] W. S. Warren, H. Rabitz, and M. Dahleh, *Science* **259**, 1581 (1993).  
[14] A. M. Weiner, *Rev. Sci. Instrum.* **71**, 1929 (2000).  
[15] T. Brabec and F. Krausz, *Rev. Mod. Phys.* **72**, 545 (2000).  
[16] S. P. Hau-Riege, R. A. London, and A. Szoke, *Phys. Rev. E* **69**, 051906 (2004).  
[17] W. R. Phillips *et al.*, *Phys. Rev. Lett.* **62**, 1025 (1989).  
[18] Y. A. Litvinov *et al.*, *Phys. Rev. Lett.* **99**, 262501 (2007).  
[19] T. Tanaka and T. Shintake, Tech. Rep., SPring-8, Riken, Japan, (2005).  
[20] M. Altarelli *et al.*, Tech. Rep. DESY 2006-097, DESY, Notkestrasse 85, p. 22607 Hamburg (2006), [http://xfel.desy.de/tdr/index\\_eng.html](http://xfel.desy.de/tdr/index_eng.html).  
[21] A. Cho, *Science* **330**, 1470 (2010).  
[22] R. Bonifacio, C. Pellegrini, and L. Narducci, *Opt. Commun.* **50**, 373 (1984).  
[23] A. T. Georges, P. Lambropoulos, and P. Zoller, *Phys. Rev. Lett.* **42**, 1609 (1979).  
[24] A. T. Georges and P. Lambropoulos, *Phys. Rev. A* **20**, 991 (1979).  
[25] J.-C. Liu *et al.*, *Phys. Rev. A* **81**, 043412 (2010).  
[26] S. Aksela *et al.*, *Phys. Rev. Lett.* **74**, 2917 (1995).  
[27] S. Svensson *et al.*, *Phys. Scr.* **14**, 141 (1976).  
[28] M. Coreno *et al.*, *Phys. Rev. A* **59**, 2494 (1999).  
[29] K. Blum, *Density Matrix Theory and Applications* (Plenum Press, New York, 1981).  
[30] G. Geloni, V. Kocharyan, and E. Saldin, [arXiv:1003.2548](https://arxiv.org/abs/1003.2548).  
[31] E. Sokell *et al.*, *J. Electron Spectrosc. Relat. Phenom.* **94**, 107 (1998).